Mechanical loading down-regulates peroxisome proliferator-activated receptor gamma in bone marrow stromal cells and favors osteoblastogenesis at the expense of adipogenesis.

Valentin David, Aline Martin, Marie-Hélène Lafage-Proust, Luc Malaval, Sylvie Peyroche, David B Jones, Laurence Vico, Alain Guignandon

Title

Mechanical loading down regulates PPARγ and favours osteoblastogenesis at the expense of adipogenesis.

Short title

Mechanical stretch as PPARγ competitor

Authors

Valentin DAVID[1‡], Aline MARTIN[1‡], Marie-Hélène LAFAGE-PROUST[1], Luc MALAVAL[1], Sylvie PEYROCHE[1], David B JONES[2], Laurence VICO[1], Alain GUIGNANDON[1*]

Affiliations

[1] INSERM E366, St-Etienne, F-42023 France ; IFR62, Lyon, F-69372, France; Université Jean Monnet, St Etienne, F-42023 France.

[2] Experimental Orthopaedics and Biomechanics, Philipps University, Baldingerst, D-35033 Marburg, Germany.

[‡] Present address: The Kidney Institute, University of Kansas Medical Center, Kansas City, KS 66160, USA

[*]**Corresponding author**

INSERM E366-LBTO, Faculté de Médecine 15 rue Ambroise Paré, F-42023 Saint-Etienne Cedex 2, France. E-mail: Alain.Guignandon@univ-st-etienne.fr

Disclosure summary: The authors have nothing to disclose

Abstract

Because a lack of mechanical information favors the development of adipocytes at the expense of osteoblasts, we hypothesized that the PPARγ-dependent balance between osteoblasts and adipocytes is affected by mechanical stimuli. We tested the robustness of this hypothesis in *in vivo* rodent osteogenic exercise, *in vitro* cyclic loading of cancellous haversian bone samples and cyclic stretching of primary stromal and C3H10T1/2 cells. We found that running rats exhibit a decreased marrow fat volume associated with an increased bone formation, presumably through recruitment of osteoprogenitors. In the tissue culture model, cyclic loading induced higher Runx2 and lower PPARγ2 protein levels. Given the pro-adipocytic and anti-osteoblastic activities of PPARγ, we studied the effects of cyclic stretching in C3H10T1/2 cells, treated either with the PPARγ activator, Rosiglitazone, or with GW9662, a potent antagonist of PPARγ. We found, through both cytochemistry and analysis of lineage marker expression, that under Roziglitazone cyclic stretch partially overcomes the induction of adipogenesis and is still able to favor osteoblast differentiation. Conversely, cyclic stretch has additive effects with GW9662 in inducing osteoblastogenesis. In conclusion, we provide evidence that mechanical stimuli are potential PPARγ modulators counteracting adipocyte differentiation and inhibition of osteoblastogenesis.

Keywords: PPARγ; Runx2; bioreactor; FlexerCell; running rats; C3H10T1/2

Introduction

The differentiation of multipotent stem-cells of mesodermal origin results in the formation of adipocytes, chondrocytes, osteoblasts and myoblasts (1-3). A shift in differentiation and survival rates from osteoblastic to adipocytic lineage could lead to an altered ratio of fat to bone cells that may, eventually, alter bone mass (4). In humans osteoporosis and age-related osteopenia were shown to be associated with an increase in marrow fat tissue (5, 6). In some of these studies osteoblast numbers correlated negatively with the number of adipocytes (5, 7, 8), suggesting that adipocytes are generated at the expense of osteoblasts. This hypothesis is supported by the isolation from the bone marrow of single cell clones that can differentiate *in vitro* into either lineage (9).

Essential to cellular commitment to a differentiation lineage is the activation of defined transcription factors (10), (11), (12). Osteoblastic differentiation is driven by runx2, followed by osterix, and then characterized by the expression of alkaline phosphatase, osteocalcin, and eventually by the mineralization of the extracellular matrix. Differentiation of adipocytes is initiated through C/EBPα and C/EBPβ that activate expression of peroxysome proliferator-activated receptor γ (PPARγ) a member of the nuclear hormone receptor family (13), (14). PPARγ regulates adipocyte-specific gene expression and is critical for the formation of mature lipid-filled adipose cells from pluripotent stem cells (15); it has also a central role in other processes such as, for example, inflammation and macrophage formation (16), (17). A recent study has demonstrated that use of the PPARγ ligands, thiazolidinediones (TZD) induces changes in bone mineral density (BMD) in elderly patients with type 2 diabetes (18), confirming the effect of TZDs (19) reported from animal models.

Among the various osteopenic animal models in which an inverse relationship was previously reported between the amount of bone marrow fat tissue and trabecular bone density are ovariectomy (20), glucocorticoid treatment (21) and also immobilization (7). Focussing on the

latter case, we hypothesized that if lack of mechanical stimuli favors the development of adipocytes at the expense of osteoblasts, the opposite might happen when external mechanical stimuli are applied. We first studied whether an osteogenic physical exercise is able to reduce bone marrow adiposity in rats. We then tested our hypothesis on lamellar bone and away from the potential confounding influence of systemic factors, by culturing bovine bovine sternum samples in a recently developed bioreactor, the ZetOS^{TM}, which allows ex vivo long term compression-loading and mechanical testing of perfused samples (22). It has been recently shown that manipulating cell tension regulates the commitment of human mesenchymal stem cells to adipocyte or osteoblast fate (23); we thus applied mechanical stretch known to alter cell tension to stromal cells extracted from the marrow of bovine bone cores and we compared their responses to the well characterized pluripotent mesenchymal stem cell line C3H10T1/2.

We show that PPARγ2 activity is modulated by mechanical conditions, strongly enough to be still responsive to mechanical stimuli even when the cells are treated by with agonist or antagonist compounds. We also demonstrate that osteo/adipo-genesis control by mechanical stimuli is not restricted to a particular cell line, a unique mechanical regimen or specific experimental conditions, since our results comprise cells of bovine and murine origin, primary and immortalized, *in vitro* and *in vivo*.

Materials and Methods

Cell culture products

Insulin, all trans retinoic acid (tRA), DAPI, oil red O, L-ascorbic acid 2-phosphate, trypsin-EDTA reagent, clostridium histolyticum neutral collagenase, p-nitrophenyl phosphate (PNP-p) were purchased from Sigma Aldrich (Lyon, France). DMEM-Ham's F-12 (DMEM/F12, 1:1, vol/vol), alpha MEM, DMEM was purchased from Eurobio (Courtaboeuf, France). Rosiglitazone and GW9662 were purchased from Interchim (Montluçon, France). Qiashedder and RNeasy mini kits were purchased from Qiagen (Courtaboeuf, France). First-strand cDNA synthesis kit for RT-PCR (AMV), Light cycler-FastStart DNA Master, SYBR Green I, and Light Cycler Instrument were purchased from Roche Diagnostics (Meylan, France). Protein assay kit (bicinchoninic acid, BCA) was obtained from Interchim (Montluçon, France).

Mesenchymal precursor cell isolation

Bovine mesenchymal stem cells (bMSC) were isolated from sternum of young males (6-8 months) and collected in sterile conditions at local slaughterhouse immediately after sacrifice. We received permission from our local ethic committee. Briefly, after removing soft tissues, sternums were reduced to 5-mm-thick fragments. The marrow was then flushed and submitted to a 15 min enzymatic digestion with 1 mg/ml clostridium histolyticum neutral collagenase at 37 °C in alpha MEM medium. Collagenase was neutralized with medium supplemented with 15% fetal calf serum (FCS). After neutralization with 15% FCS, the marrow was resuspended in Eagle's medium supplemented with 10% FCS (Sigma Aldrich, Lyon, France), 2 mM L-Glutamine, and 1% antibiotics (50 U/ml penicillin and 50 µg/ml streptomycin) and plated at 5000 cells/cm². The medium was changed after the first 24 h to remove non-adherent cells.

Cell culture

Cells were grown in tissue culture T75-flask (Elvetec, France) in 5% CO2 humidified atmosphere at 37 °C. The mouse pluripotent mesenchymal stem cell line C3H10T1/2 (clone-8, American Type Culture Collection, LGC Promochem, Molsheim, France) was cultured in α-minimum Eagle's medium, whereas bovine mesenchymal stem cells (bMSC) were cultured in DMEM, supplemented with 10% FCS (PromoCell GMBH, Heidelberg, Germany), L-Glutamine, and antibiotics as above. After reaching a subconfluent state, cells were trypsinized with 1x trypsin-EDTA and plated onto flexible type I collagen-coated, silicon-bottom, six-well culture plates (Bioflex; Flexcell Corp., McKeesport, PA), at 2500 cell/cm² for C3H10T1/2 and 5000 cell/cm² for BMSC and the medium was changed every other day.

Mechanical stretching

Starting 72 hours after seeding (referred to as Day 0) cells were subjected to daily mechanical deformation during 2 weeks. Mechanical deformation was induced with a Flexcell Strain Unit Fx-3000 (Flexcell Corp., Hillsborough, NC, US) (24), which consists of a vacuum manifold regulated by solenoid valves that are controlled by a computer timer program. Each plate is inserted over six buttons in the Bioflex loading station. Application, through an air pump, of a negative pressure of 80 kilopascals stretches horizontally the bottom of the culture plate over the plastic button. Thus, 85% of the surface of the flexible wells is submitted to a known percentage of uniform elongation. The membranes are then released to their original conformation (24). The experimental regimen used in this study delivered 4000 με elongation at 1Hz frequency (triangular signal) during 300 cycles per day. Stretched cells remained adherent, and the deformation of the membrane was directly transmitted to the cells. Unstretched cells grown on Bioflex plates were used as controls. Starting from Day 0 media were supplemented with 10% FCS (PromoCell GMBH, Heidelberg, Germany), 50 µg/ml ascorbic acid, 10^{-6}M β-glycerophosphate, 10^{-8} M all trans-retinoic acid, 10^{-8} M Dexametasone (Dex), 1% Insulin, 5.10^{-5}

M 3-isobutyl-1-methylxanthine (IBMX) to create conditions inducing both osteoblastic and adipogenic cells. The differentiation into various cell lineages is regulated by factors such as cytokines and growth hormones, cAMP-elevating agents and ligands for members of the steroid/thyroid receptor-gene family of transcription factors (25), (26). Among these factors, all tRA has been reported to increase the expression of osteoblastic-related cell markers such as alkaline phosphatase (27), (28).

PPARγ induction and inhibition

To evaluate the involvement of PPARγ in the response to mechanical stretching, cells were treated during the culture period with 1µM (EC50; Kd 43 Nm) of a powerful agonist of PPARγ, BRL49653 or Rosiglitazone or DMSO as a vehicle. PPARγ activation was inhibited with 1 µM (EC50) of an antagonist of PPARγ, GW9662. The compounds were added to the culture medium at Day 0, and renewed every two days.

Histochemical staining

After 2% formaldehyde and rinsing, the activity of the plasma membrane-associated alkaline phosphatase was detected using an Alkaline Phosphatase Leukocyte Staining Kit (Sigma Aldrich, Lyon, France), according to the manufacturer's protocol. The cultures were then rinsed three times for 5 min in deionized water and cytoplasmic triglyceride droplets were stained with oil-red O (29). Nuclei were stained with DAPI. The percent of alkaline phosphatase and oil-Red O-positive cells was determined by counting cells in 30 contiguous fields/well after random starts.

Protein extraction

Total proteins were extracted in 2 mL lysis buffer/well containing 10 mL/L Nonidet 40, 1.8 g/L Iodoacetamide, 3.5 mL/L PIC (proteases inhibition cocktail, Sigma Aldrich, Lyon, France) and 2 µL/L β-mercaptoethanol. After centrifugation (5 min, 5000 rpm, 4°C), supernatants were stored at -20°C. Cytoplasmic and nuclear protein fractions were separated using a nuclear extraction

kit (Active Motif, Rixensart, Belgium). Briefly, cells were scrapped-collected in 3 ml ice-cold PBS-Phosphatase Inhibitors cocktail, the material was kept at 4°C thereafter. The cell suspension was spun for 5 minutes at 500 rpm. The pellet was resuspended in 500 µl Hypotonic Buffer and incubated for 15 minutes on ice. Cell membranes were lysed with 25 µl detergent. The cytoplasmic protein fraction was collected after a 30 seconds spin at 14,000g. Nuclear pellets were resuspended in 50 µl lysis buffer then incubated for 30 minutes on ice on a rocking platform at 150 rpm. The suspension was then spun for 10 minutes at 14,000g and the nuclear fraction (supernatant) was collected in microcentrifuge tube. Aliquots were store at –80ºC. Protein concentration was measured using the bicinchoninic acid (BCA) protein assay kit (Pierce, Perbio Science France SAS, Brebières, France).

Alkaline phosphatase assay

Alkaline phosphatase activity (ALP) was measured by assessing the hydrolysis of p-nitrophenyl phosphate (PNP-p) in inorganic phosphate (Pi) at 37°C. Briefly, the assay mixture consisted of 100-µl cell homogenate and 900-µl reaction mixture (2 mM PNP-p, 2 mM MgCl2, 2-amino-2-Methyl-1-Propanol 95%, pH 10.5). The reaction was initiated by the addition of the cell extract and product amounts were read after 50 min at 412 nm on a spectrophotometer. ALP was expressed as nmol Pi/mg protein/min.

Sandwich ELISA

Sandwich ELISAS were designed in our laboratory to quantify PPARγ2, and Runx2 in protein extracts. A capture antibody [runx2; Rabbit anti-human (CBFA11-A, 4ADI, TEBU) and PPARγ; Rabbit IgG anti-mouse (PA1-824, ABR, TEBU)] is first coated on each well in 0.1M Bicarbonate buffer, pH 9.2, overnight at 4°C. The wells are then blocked for 60 min at room temperature in 100 µl of 100 mM phosphate buffer, pH 7.2, 1% bovine serum albumin (BSA) and 0.5% Tween-20). After 3 washes in wash buffer (100 mM phosphate buffer, 150 mM NaCl, 0.2% BSA and

0.05% Tween 20), samples or standards are added to the plates in 100 µl/well. Plates are then incubated at room temperature for one hour then overnight at 4°C. After wash, 100µl of the second antibody [runx 2; Goat anti-human (sc-12488, TEBU) and PPARγ; Goat anti-human (sc-6284, TEBU)] are added to each well and incubated at room temperature for 4 hours. The plates are washed, and an ALP-labeled secondary antibody [Rabbit IgG anti goat (Zymed)] is added to each well and incubated at room temperature for 4 hours. After wash, fast pNP enzyme substrate (Sigma Aldrich, Lyon, France) is added to the wells and incubated for 30 minutes. Color intensities are measured at 412 nm with a spectrophotometer, using a blank reference. Antigen concentrations are determined from a calibration curve using serial dilution of an arbitrary sample as standards.

PPARγ activity measurement

DNA binding PPARγ activity was determined using the ELISA-based PPARγ activation TransAM™ kit (Active Motif, Rixensart, Belgium). PPARγ contained in nuclear extracts bind specifically to an oligonucleotide containing the Peroxisome Proliferator Response Element (PPRE 5´-AACTAGGTCAAAGGTCA-3´) and are detected with an anti PPARγ antibody. A secondary antibody conjugated to horseradish peroxidase provides a sensitive colorimetric readout that is quantified by spectrophotometry at 405 nm.

RNA extraction, RT and Real time PCR

RNA extraction was performed on cells at various time points up to 14 days after the beginning of stimulation. Total RNA was isolated by guanidium isothiocyanate extraction using the RNeasy mini kit according to manufacturer's instruction. Briefly, the samples were disrupted in lysis buffer containing guanidium isothiocyanate and homogenized using Qiashedder. The samples were then applied to the RNeasy spin column and total RNAs bound to the membrane were eluted in water. Integrity of RNA was checked by electrophoresis, after ethidium bromide

staining. RNAs were reverse-transcribed into single-stranded cDNA using first strand cDNA synthesis kit for RT-PCR (AMV) from 2 µg total RNA in a 20 µl reaction mix containing 2 µl of 10× reaction, 5 mM MgCl2, 20 mmol each of dNTP, 50 pmol of oligo-p(dT)15 primer, 50 U of RNase inhibitor, and 20 U of AMV reverse transcriptase. The reaction was incubated for 60 min at 42°C. The single strand cDNA was diluted 1:10 and 8µl were amplified with a LightCycler (Roche Diagnosticcs, Meylan, France) in 20µl PCR mixture containing 2µL of Light cycler-FastStart DNA Master SYBR Green I, 3mM MgCl2, 0.5µM of 5' and 3' oligo-primers and water. A typical protocol included a denaturation step at 95°C for 10 min followed by 40 cycles with 95°C for 1 s, Tm°C annealing for A s, and Te°C extension for M s. The fluorescence product was detected at the end of the extension period after a 60s at 60°C. θm, A, Tm, D, M, X, E, primers and product length are summarized in **Table 1**. Quantified data were analyzed with the Light-Cycler analysis software. Serial dilution of total RNA was performed from 16 ng to 0.25 ng, and used as standards. For realtime PCR assay, 2–4 ng of input RNA was used. Results were analyzed following the manufacturer's instructions: (a) checking the PCR products specificity and (b) calculating the variation in PCR products concentration between experimental groups, expressed as percentage of mean control values.

Ex vivo studies

Cancellous bovine bone was used because it presented similar architecture as human trabecular bone and have been successfully used as xenografts to repair bony defects (30). Cancellous bovine bone was isolated from sternum of young males (6-8 months), machined with high precision to cylindrical cores (10 mm diameter, 5 mm height) under sterile conditions, and inserted into the loading chambers of a Zetos^{TM} bone perfusion system (22). Each core was maintained at 37°C and perfused with 5 ml DMEM Ham F12 (1:1), recirculating at a rate of 6 ml/h. Half of the bone samples were subjected to 300 cycles daily mechanical compression at 1Hz, 4000 µε amplitude (similar to FlexerCell protocol), the other half were unloaded controls.

Five loaded and five unloaded bones were collected at day 7, 14 and 21 and the protein fraction was collected (see protein extraction section).

In vivo study

Nine-week young adult male Wistar rats were used for the experiment. Animals were kept in the laboratory for one week before the experiment to allow acclimatization to the diet and new environment. The light/dark cycle was 12 h with lights on from 7:00 to 19:00 hours. The rats were allowed free access to water and chow diet. The rats were trained on a treadmill at 60% of maximal O_2 consumption, 5 days per week. VO_{2max} was determined on the open-flow system apparatus as described in Bourrin et al. (31). Briefly, the rats ran on a treadmill placed in a closed Plexiglas chamber with a controlled and measured air flow. After acclimatization to the new environment, the rats were trained to obtain a maximal exercise. The O_2 and CO_2 expired were measured and recorded every 3 minutes while the animal is exercising. On the first day, rats of the exercise group ran 15 minutes at a speed of 20m/minute on the treadmill being maintained horizontal. Thereafter, the duration of each training session was progressively increased until the animals ran 1 hour and 30 minutes per day at a speed of 20m/minute after 1 week of training. By the fifth week of training, rats ran 1 hour and 30 minutes per day at a speed of 30m/min on the level. At the end of the experiment, rats were injected with fluorochromes twice (6 days apart) in order to measure the dynamic parameters of bone formation. The bone effects of this training program were published elsewhere (31). Tibiae from 20 male Wistar rats, ten sedentary control rats and ten running animals from the study of Bourrin et al. (31) were analyzed by histology. The proximal tibia metaphysis were fixed in 4% formaldehyde solution, dehydrated in acetone and embedded in methylmethacrylate. Longitudinal frontal slices were cut from the embedded bones with a Jung Model K microtome (Carl Zeiss, Heidelberg, Germany). Six non-serial sections, 8 µm thick, were used for modified Goldner staining. The relative volume of fat in the marrow cavity (Ad.V/MV) was measured on Goldner sections using a manual counter and a hundred-point grid according to (32).

Statistical analysis

Statistical analysis was performed using the STATISTICA software (StatSoft Inc., Tulsa, OK, USA). One way or two ways analysis of variance (ANOVA) was performed on protein and RNA data. When F values for a given variable were found to be significant, the sequentially rejecting Bonferroni-Holm test (33) was subsequently performed using the Holm's adjusted p-values taken from the t table. Results were considered to be significantly different at $p<0.05$. The Mann-Whitney U test was used to compare histomorphometry data.

Results

Osteogenic physical exercise reduces marrow fat in male rat tibia metaphysis in vivo

Over 5 weeks of training, treadmill-running rats at 60% of their maximal O_2 consumption display a 33% increase of bone formation rate (**Figure 1A**) and a 18% decrease of bone resorption (not shown, see (31)). The mineral apposition rate relative to osteoblastic activity is unaltered (not shown), suggesting that osteoblastic recruitment is stimulated (31). Mechanical stimulation also decreases adipocyte number (Ad.Ar/T.Ar) by 39% in running rats (**Figure 1B**), showing that the balance between osteoblasts and adipocytes is modulated by mechanical stimulation.

Cyclic mechanical compression increases Runx2 and decreases PPARγ2 protein levels in bovine cancellous bone cores cultivated *ex vivo*.

We evaluated the effects of a loading regimen on Runx2 and PPARγ expression in sternum bovine cylindrical bone cores submitted to cyclic compression. We used an accurate mechanical loading system combined with a trabecular bone culture-loading chamber, the Zetos™ (22), which provides the ability to study trabecular bone under controlled culture and loading conditions over 3 weeks. We have previously shown that daily cyclic compression of cancellous bone in this device results in increased bone formation rate, leading to thicker trabeculae and higher Young's Modulus (David et al., submitted). Here we show that daily cyclic mechanical compression increases Runx2 protein levels after 7 and 14 days (**Figure 2A**). In contrast, PPARγ2 levels decrease after 21 days in loaded samples as compared to baseline values (**Figure 2B**). In unloaded control samples PPARγ2 protein expression remain stable over the 21-day culture period.

In vitro, mechanical stretching of multipotent mesenchymal progenitors results in more osteoblasts and less adipocytes

When grown under static conditions, in permissive osteoblastic/adipocytic media, 45% of C3H10T1/2 cells become alkaline phosphatase positive and 27 % oil red O positive after 14 days, while the figures are 34% and 10%, respectively, in bMSC grown for 21 days.

In bMSC, at day 21, mechanical stretching increases the percent of alkaline phosphatase-positive cells (38±2.8% vs. 33±3.1%, $p<0.05$) and decreases the proportion of oil-redO-positive cells (6±3% vs. 10±2.5%, $p<0.05$). Furthermore, at day 14, alkaline phosphatase activity is greatly increased in stretched bMSC cells, as compared to unstretched controls (**Figure 3A**). Daily mechanical stretching induces a strong increase in Runx2 protein amounts at day 7 and of osteocalcin protein content at day 14 (**Figure 3B**). Consistent with these findings, *runx2* and *osx* transcripts are greatly increased at day 7 and 14 in stretched cells, as well as osteocalcin mRNA levels at day 14 (**Figure 3C**). In contrast, PPARγ2 protein levels (**Figure 3B**, day 14) and mRNA (day 7), as well as *aP2* mRNA (day 14) decrease in stretched cultures (**Figure 3C**).

PPARγ is involved in the mechanical-regulated balance between osteoblasts and adipocytes

It has been shown that PPARγ insufficiency stimulates osteoblastogenesis from bone marrow progenitors (36). We evaluated the role of PPARγ in mechanically stretched C3H10T1/2 cells. Unstretched and stretched cells were treated either with Rosiglitazone, a potent PPARγ agonist or with GW9662, a selective PPARγ antagonist. As expected, Rosiglitazone greatly increased and GW9662 reduced the number of differentiated adipocytes (oil-red O-positive cells) after 14 days (**Figure 4A**). Fourteen days of mechanical stretching increase osteoblast differentiation as assessed by the percent of alkaline phosphatase-positive cells (**Figure 4B**). Conversely, adipogenic differentiation is decreased in stretched cultures (**Figure 4C**). Interestingly, in

GW9662 treated cells, stretching increases the number of alkaline phosphatase-positive cells (**Figure 4B**), and is still able to decrease adipocyte numbers under rosiglitazone treatment (**Figure 4C**). This is reflected in marker expression. Mechanical stretch increases gene expression of *Runx2* at day 3 (not shown), 7 and 14 (**Figure 5A**). Rosiglitazone and GW9662 treatment decrease the expression of *Runx2* markers in unstretched conditions. GW9662 at days 7 and 14 and rosiglitazone at day 7 do not impair stretch–induced *Runx2* stimulation (**Figure 5A**). Rosiglitazone treatment increases gene expression of adipogenic markers such as *ADD1/Srebp1* at day 7 (not shown), *PPARγ2* at days 7 and 14 (**Figure 5B**) and *aP2* at day 14 (not shown). As expected, expression of these genes is inhibited under GW9662 treatment. Interestingly, mechanical stretch is still able to reduce *PPARγ2 mRNA* expression (**Figure 5B**), as well as *ADD1/Srebp1, aP2* and *adipsin* expression (not shown), in both agonist and antagonist conditions. This suggests that mechanical stretch acts as a PPARγ antagonist.

Mechanical stretch as PPARγ antagonist

In order to better characterise the effect of mechanical stretch as a modulator of PPARγ action, we studied the location and activity of Runx2 and of PPARγ proteins. Fourteen days of mechanical stretch increase nuclear Runx2 protein content in C3H10T1/2cultures (**Figure 6A)**. Rosiglitazone and GW9662 treatment do do not affect nuclear Runx2, but Rosiglitazone abolishes the effect of stretching, while GW9662 induces a 75% increase in Runx2 content above stretched controls (**Figure 6A**). Mechanical stretch decreases nuclear PPARγ2 protein content (**Figure 6B**) and PPARγ DNA binding (**Figure 6C**) after 7days, demonstrating the inhibitory effect of mechanical stimulation on PPARγ transcriptional activity. As expected, 7 days of Rosiglitazone treatment alone increase PPARγ2 protein expression (**Figure 6B**) and PPARγ DNA binding activity (**Figure 6C**). Interestingly, in Rosiglitazone-treated cells stretching decreases nuclear PPARγ amounts (**Figure 6B**) and significantly reduces PPARγ DNA binding (**Figure 6C**). Seven days of GW9662 treatment decrease PPARγ2 protein content in the cytoplasm, (not shown) and the nucleus (**Figures 6B)** as well as PPARγ DNA binding activity

(**Figure 6C**). Stretching of GW9662-treated cells induces a further decrease of PPARγ2 nuclear protein content (**Figure 6B**) while no additive effect of stretch is detected on the residual level of PPARγ DNA binding (**Figure 6C**).

Discussion

Five weeks of osteogenic treadmill running induce in rats a higher bone formation resulting from increased mineralising surfaces, i.e. active osteoblasts, and mirrored by lower adipocyte numbers in the bone marrow. Similarly, in a bone core explant dynamic culture system, we found that Runx2 protein levels are enhanced in compression-loaded samples, whereas PPARγ2 protein levels are decreased. Those results obtained on different species, with lamellar (bovine) and non-lamellar (rodent) bone and for different mechanical activities emphasize the fact that local mechanical signals are strong actors of the osteoblast/adipocyte balance. Very few studies have investigated the effects of mechanical stretch on uncommitted cells, whereas it has been shown that mechanical loading triggers an increase in intramedullary pressure as well as streaming potentials (37), therefore providing mechanical signals for multipotent progenitor in vivo (38). We thus applied mechanical stimuli to bMSC and the pluripotent mesenchymal stem cell line C3H10T1/2 grown under media permissive for both osteoblast and adipocyte differentiation. Our results show that mechanical stretch results in more osteoblasts both in primary bMSC. Up-regulation of protein and mRNA levels of Runx2 was seen in both models and Runx2 was also elevated in strained bovine cores. Runx2 was already reported to be stimulated by mechanical stress in several models such as human spinal ligament cells (39) and human preosteoblasts (40). The regulation of this transcription factor, expressed by mesenchymal stem cells prior to cell differentiation, by preosteoblasts, terminally differentiated osteoblasts and prehypertrophic chondrocytes (41) occurs as early as the third day of stretching, suggesting that early stages of culture might be also responsive to mechanical stimuli. Alkaline phosphatase activity, an early marker of the osteoblastic lineage, osterix which is expressed later and osteocalcin, a marker of mature osteoblasts, were all stimulated by mechanical stretching in a time course that matches osteoblastic differentiation kinetics. Furthermore, osteoblast numbers were higher in stretched than in static conditions.

Cyclic stretch has been recently shown to reduce adipocyte differentiation in the mouse preadipocyte 3T3-L1 cell line (42), providing the first evidence for a direct effect of mechanical stimuli on fat cells. Interestingly, this effect was the result of the down regulation of PPARγ2 by stretched-induced ERK activation. We (43) and others (44) previously showed that mechanical strain exerts its stimulating effects on osteoblasts through ERK activation. Thus, the MAPK signaling pathway appears as one of the potential molecular links modulating the osteoblast/adipocyte balance. We showed both *in vivo* and *in vitro* that lipid droplets, the hallmark of the adipocyte phenotype are decreased by mechanical stretch. The control of adipogenesis involves the interaction of a number of intracellular signaling pathways and the activation of numerous transcription factors (45), (46), particularly PPARγ (26). Mounting evidence indicates an important role of PPARγ in skeletal metabolism. Specifically, PPARγ haploinsufficient mice exhibit increased bone mass associated with increased osteoblastogenesis and decreased adipogenesis. Our experiments, both *in vitro* and *ex vivo*, indicate that inhibition of PPARγ2 -the most potent adipogenic isoform *in vitro* (47)- is part of the mechanism whereby mechanical stretch inhibits adipogenesis and stimulates osteoblastogenesis. In bMSC cultures, mechanical stretch reduced PPARγ2 and protein levels. Mechanical stretch-induced PPARγ2 inhibition was followed by decreased expression of *aP2*, a late marker of adipocyte differentiation. Similar effects were found in C3H10T1/2 cells. In addition we found that the reduction in PPARγ2 amounts in nuclear and cytoplasmic fractions was paralleled by a reduction in PPARγ nuclear activity. That the expression of ADD1/SREBP1 was decreased in stretched conditions provides a plausible explanation for PPARγ loss of activity, as transactivation of the PPARγ promoter depends on transcription factors such as add1/serbp1 (48).

Thiazolidinediones (TZDs), a novel class of antidiabetic agents that acts as insulin sensitizers *in vivo*, bind PPARγ with high affinity. PPARγ regulates target gene transcription as an heterodimer with the retinoid X receptor, and this heterodimeric complex has been shown to be activated synergistically by TZDs and RXR-specific ligands (49). TZDs enhance adipogenesis in

stromal cells (50). Activation of PPARγ by Rosiglitazone has been shown to stimulate adipogenesis and inhibits osteoblastogenesis in murine bone marrow-derived clonal cell line (51) and in mice, with an associated bone loss (52), (19), an action that we confirm in the murine C3H10T1/2 cell line. Mechanical stretch applied to Rosiglitazone-treated cultures was able to counteract the increase of PPARγ expression and activity. Moreover, in Rosiglitazone-treated cells mechanical stretch was still efficient in promoting osteoblastogenesis. On the other hand, combining GW9662 treatment and mechanical stretching had additive effects on osteoblast numbers and Runx2 expression. These results emphasize the power of mechanical stretch in promoting osteoblastogenesis. Thus, mechanical signals are potential PPARγ modulators counteracting adipocyte overdifferentiation and osteoblastogenesis inhibition, as summarized in **Figure 7**.

Conclusions

Overall, our findings show that mechanical stimuli have a pivotal role in modifying the osteoblasto-/adipo-genesis balance in different species, at the cell, tissue and organism levels, by challenging two key transcription factors, Runx2 and PPARγ, which are strongly interdependent in serving osteoblastogenesis or adipogenesis. These results provide new insights into a physiological mechanism by which physical exercise might promote bone formation. Controversial duality of PPARγ as a therapeutic target for obesity-associated insulin resistance on the one hand, and as an adipogenic determination factor that might lead to osteopenia on the other hand, has to be clarified. Nevertheless, our data suggest that osteoblastogenesis, when inhibited secondary to TZD treatment, could be in part restored by a cyclic mechanical regimen.

Acknowledgements

This study was supported by the European Space Agency: European Research In Space and Terrestrial Osteoporosis (ERISTO) contract number 14232/NL/SH (CCN3) and Microgravity Program AO-99-122 contract number 14426, and by the Institut National de la Santé et de la Recherche Médicale within the "ATC vieillissement 2002" program. The authors thank Dr Christian DANI (UMR 6543 CNRS/Université de Nice Sophia-Antipolis) for helpful discussion.

Bibliography

1. **Reznikoff CA, Brankow DW, Heidelberger C** 1973 Establishment and characterization of a cloned line of C3H mouse embryo cells sensitive to postconfluence inhibition of division. Cancer Res 33:3231-8
2. **Muraglia A, Cancedda R, Quarto R** 2000 Clonal mesenchymal progenitors from human bone marrow differentiate in vitro according to a hierarchical model. J Cell Sci 113 (Pt 7):1161-6
3. **Satomura K, Krebsbach P, Bianco P, Gehron Robey P** 2000 Osteogenic imprinting upstream of marrow stromal cell differentiation. J Cell Biochem 78:391-403
4. **Pittenger MF, Mackay AM, Beck SC, Jaiswal RK, Douglas R, Mosca JD, Moorman MA, Simonetti DW, Craig S, Marshak DR** 1999 Multilineage potential of adult human mesenchymal stem cells. Science 284:143-7
5. **Meunier P, Aaron J, Edouard C, Vignon G** 1971 Osteoporosis and the replacement of cell populations of the marrow by adipose tissue. A quantitative study of 84 iliac bone biopsies. Clin Orthop Relat Res 80:147-54
6. **Burkhardt R, Kettner G, Bohm W, Schmidmeier M, Schlag R, Frisch B, Mallmann B, Eisenmenger W, Gilg T** 1987 Changes in trabecular bone, hematopoiesis and bone marrow vessels in aplastic anemia, primary osteoporosis, and old age: a comparative histomorphometric study. Bone 8:157-64
7. **Ahdjoudj S, Lasmoles F, Holy X, Zerath E, Marie PJ** 2002 Transforming growth factor beta2 inhibits adipocyte differentiation induced by skeletal unloading in rat bone marrow stroma. J Bone Miner Res 17:668-77
8. **Benayahu D, Shur I, Ben-Eliyahu S** 2000 Hormonal changes affect the bone and bone marrow cells in a rat model. J Cell Biochem 79:407-15
9. **Park SR, Oreffo RO, Triffitt JT** 1999 Interconversion potential of cloned human marrow adipocytes in vitro. Bone 24:549-54
10. **de Crombrugghe B, Lefebvre V, Behringer RR, Bi W, Murakami S, Huang W** 2000 Transcriptional mechanisms of chondrocyte differentiation. Matrix Biol 19:389-94
11. **Rosen ED, Spiegelman BM** 2000 Molecular regulation of adipogenesis. Annu Rev Cell Dev Biol 16:145-71
12. **Wagner EF, Karsenty G** 2001 Genetic control of skeletal development. Curr Opin Genet Dev 11:527-32
13. **Wu Z, Bucher NL, Farmer SR** 1996 Induction of peroxisome proliferator-activated receptor gamma during the conversion of 3T3 fibroblasts into adipocytes is mediated by C/EBPbeta, C/EBPdelta, and glucocorticoids. Mol Cell Biol 16:4128-36
14. **Clarke SL, Robinson CE, Gimble JM** 1997 CAAT/enhancer binding proteins directly modulate transcription from the peroxisome proliferator-activated receptor gamma 2 promoter. Biochem Biophys Res Commun 240:99-103
15. **Vernochet C, Milstone DS, Iehle C, Belmonte N, Phillips B, Wdziekonski B, Villageois P, Amri EZ, O'Donnell PE, Mortensen RM, Ailhaud G, Dani C** 2002 PPARgamma-dependent and PPARgamma-independent effects on the development of adipose cells from embryonic stem cells. FEBS Lett 510:94-8
16. **Jiang C, Ting AT, Seed B** 1998 PPAR-gamma agonists inhibit production of monocyte inflammatory cytokines. Nature 391:82-6

17. **Nagy L, Tontonoz P, Alvarez JG, Chen H, Evans RM** 1998 Oxidized LDL regulates macrophage gene expression through ligand activation of PPARgamma. Cell 93:229-40
18. **Schwartz AV, Sellmeyer DE, Vittinghoff E, Palermo L, Lecka-Czernik B, Feingold KR, Strotmeyer ES, Resnick HE, Carbone L, Beamer BA, Won Park S, Lane NE, Harris TB, Cummings SR** 2006 Thiazolidinedione (TZD) Use and Bone Loss in Older Diabetic Adults. J Clin Endocrinol Metab
19. **Rzonca SO, Suva LJ, Gaddy D, Montague DC, Lecka-Czernik B** 2004 Bone is a target for the antidiabetic compound rosiglitazone. Endocrinology 145:401-6
20. **Martin RB, Zissimos SL** 1991 Relationships between marrow fat and bone turnover in ovariectomized and intact rats. Bone 12:123-31
21. **Wang GJ, Sweet DE, Reger SI, Thompson RC** 1977 Fat-cell changes as a mechanism of avascular necrosis of the femoral head in cortisone-treated rabbits. J Bone Joint Surg Am 59:729-35
22. **Jones DB, Broeckmann E, Pohl T, Smith EL** 2003 Development of a mechanical testing and loading system for trabecular bone studies for long term culture. Eur Cell Mater 5:48-59; discussion 59-60
23. **McBeath R, Pirone DM, Nelson CM, Bhadriraju K, Chen CS** 2004 Cell shape, cytoskeletal tension, and RhoA regulate stem cell lineage commitment. Dev Cell 6:483-95
24. **Banes AJ, Gilbert J, Taylor D, Monbureau O** 1985 A new vacuum-operated stress-providing instrument that applies static or variable duration cyclic tension or compression to cells in vitro. J Cell Sci 75:35-42
25. **Sul HS** 1989 Adipocyte differentiation and gene expression. Curr Opin Cell Biol 1:1116-21
26. **Spiegelman BM** 1998 PPAR-gamma: adipogenic regulator and thiazolidinedione receptor. Diabetes 47:507-14
27. **Benayahu D, Fried A, Wientroub S** 1995 PTH and 1,25(OH)2 vitamin D priming to growth factors differentially regulates the osteoblastic markers in MBA-15 clonal subpopulations. Biochem Biophys Res Commun 210:197-204
28. **Choong PF, Martin TJ, Ng KW** 1993 Effects of ascorbic acid, calcitriol, and retinoic acid on the differentiation of preosteoblasts. J Orthop Res 11:638-47
29. **Novikoff AB, Novikoff PM, Rosen OM, Rubin CS** 1980 Organelle relationships in cultured 3T3-L1 preadipocytes. J Cell Biol 87:180-96
30. **Liebschner MA** 2004 Biomechanical considerations of animal models used in tissue engineering of bone. Biomaterials 25:1697-714
31. **Bourrin S, Palle S, Pupier R, Vico L, Alexandre C** 1995 Effect of physical training on bone adaptation in three zones of the rat tibia. J Bone Miner Res 10:1745-52
32. **Martin A, de Vittoris R, David V, Moraes R, Begeot M, Lafage-Proust MH, Alexandre C, Vico L, Thomas T** 2005 Leptin modulates both resorption and formation while preventing disuse-induced bone loss in tail-suspended female rats. Endocrinology 146:3652-9
33. **Holm S** 1979 A simple sequentially rejective multiple test procedure. Scand J Stat 6:65-70
34. **Katagiri T, Yamaguchi A, Ikeda T, Yoshiki S, Wozney JM, Rosen V, Wang EA, Tanaka H, Omura S, Suda T** 1990 The non-osteogenic mouse pluripotent cell line, C3H10T1/2, is induced to differentiate into osteoblastic cells by recombinant human bone morphogenetic protein-2. Biochem Biophys Res Commun 172:295-9
35. **Lehmann JM, Moore LB, Smith-Oliver TA, Wilkison WO, Willson TM, Kliewer SA** 1995 An antidiabetic thiazolidinedione is a high affinity ligand for

peroxisome proliferator-activated receptor gamma (PPAR gamma). J Biol Chem 270:12953-6

36. **Akune T, Ohba S, Kamekura S, Yamaguchi M, Chung UI, Kubota N, Terauchi Y, Harada Y, Azuma Y, Nakamura K, Kadowaki T, Kawaguchi H** 2004 PPARgamma insufficiency enhances osteogenesis through osteoblast formation from bone marrow progenitors. J Clin Invest 113:846-55
37. **Qin YX, Lin W, Rubin C** 2002 The pathway of bone fluid flow as defined by in vivo intramedullary pressure and streaming potential measurements. Ann Biomed Eng 30:693-702
38. **Qin YX, Kaplan T, Saldanha A, Rubin C** 2003 Fluid pressure gradients, arising from oscillations in intramedullary pressure, is correlated with the formation of bone and inhibition of intracortical porosity. J Biomech 36:1427-37
39. **Iwasaki K, Furukawa KI, Tanno M, Kusumi T, Ueyama K, Tanaka M, Kudo H, Toh S, Harata S, Motomura S** 2004 Uni-axial cyclic stretch induces Cbfa1 expression in spinal ligament cells derived from patients with ossification of the posterior longitudinal ligament. Calcif Tissue Int 74:448-57
40. **Yuge L, Okubo A, Miyashita T, Kumagai T, Nikawa T, Takeda S, Kanno M, Urabe Y, Sugiyama M, Kataoka K** 2003 Physical stress by magnetic force accelerates differentiation of human osteoblasts. Biochem Biophys Res Commun 311:32-8
41. **Geoffroy V, Kneissel M, Fournier B, Boyde A, Matthias P** 2002 High bone resorption in adult aging transgenic mice overexpressing cbfa1/runx2 in cells of the osteoblastic lineage. Mol Cell Biol 22:6222-33
42. **Tanabe Y, Koga M, Saito M, Matsunaga Y, Nakayama K** 2004 Inhibition of adipocyte differentiation by mechanical stretching through ERK-mediated downregulation of PPARgamma2. J Cell Sci 117:3605-14
43. **Boutahar N, Guignandon A, Vico L, Lafage-Proust MH** 2004 Mechanical strain on osteoblasts activates autophosphorylation of focal adhesion kinase and proline-rich tyrosine kinase 2 tyrosine sites involved in ERK activation. J Biol Chem 279:30588-99
44. **Yang CM, Chien CS, Yao CC, Hsiao LD, Huang YC, Wu CB** 2004 Mechanical strain induces collagenase-3 (MMP-13) expression in MC3T3-E1 osteoblastic cells. J Biol Chem 279:22158-65
45. **Ntambi JM, Young-Cheul K** 2000 Adipocyte differentiation and gene expression. J Nutr 130:3122S-3126S
46. **McDougall K, Beecroft J, Wasnidge C, King WA, Hahnel A** 1998 Sequences and expression patterns of alkaline phosphatase isozymes in preattachment bovine embryos and the adult bovine. Mol Reprod Dev 50:7-17
47. **Medina-Gomez G, Virtue S, Lelliott C, Boiani R, Campbell M, Christodoulides C, Perrin C, Jimenez-Linan M, Blount M, Dixon J, Zahn D, Thresher RR, Aparicio S, Carlton M, Colledge WH, Kettunen MI, Seppanen-Laakso T, Sethi JK, O'Rahilly S, Brindle K, Cinti S, Oresic M, Burcelin R, Vidal-Puig A** 2005 The link between nutritional status and insulin sensitivity is dependent on the adipocyte-specific peroxisome proliferator-activated receptor-gamma2 isoform. Diabetes 54:1706-16
48. **Miard S, Fajas L** 2005 Atypical transcriptional regulators and cofactors of PPARgamma. Int J Obes (Lond) 29 Suppl 1:S10-2
49. **Mukherjee R, Davies PJ, Crombie DL, Bischoff ED, Cesario RM, Jow L, Hamann LG, Boehm MF, Mondon CE, Nadzan AM, Paterniti JR, Jr., Heyman RA** 1997 Sensitization of diabetic and obese mice to insulin by retinoid X receptor agonists. Nature 386:407-10

50. **Gimble JM, Robinson CE, Wu X, Kelly KA, Rodriguez BR, Kliewer SA, Lehmann JM, Morris DC** 1996 Peroxisome proliferator-activated receptor-gamma activation by thiazolidinediones induces adipogenesis in bone marrow stromal cells. Mol Pharmacol 50:1087-94
51. **Lecka-Czernik B, Gubrij I, Moerman EJ, Kajkenova O, Lipschitz DA, Manolagas SC, Jilka RL** 1999 Inhibition of Osf2/Cbfa1 expression and terminal osteoblast differentiation by PPARgamma2. J Cell Biochem 74:357-71
52. **Ali AA, Weinstein RS, Stewart SA, Parfitt AM, Manolagas SC, Jilka RL** 2005 Rosiglitazone causes bone loss in mice by suppressing osteoblast differentiation and bone formation. Endocrinology 146:1226-35

Figure legends

Figure 1.
Effects of physical exercise on bone formation rate [BFR] (**A**) and marrow adipocyte volume [Ad.Ar/T.Ar] (**B**) in the proximal tibia metaphysis of 5-week treadmill-running trained rats. Animals were either sedentary controls (open boxes) or running (stripped boxes) in a treadmill. Values are box plots of 10 samples per group. *: $p<0.05$ vs. Sedentary, Mann-Whitney U test.

Figure 2.
Effects of cyclic mechanical compression of sternum bone cores in the Zetos™ organotypic system on Runx2 (**A**) and PPARγ2 (**B**) protein contents. Samples were either unloaded (open bars) or loaded once a day for 5 minutes (stripped bars). Values are mean ± SEM of 5 samples (bone cores) per group expressed as a percentage of unloaded control at day 7. *: $p<0.05$ vs matched unloaded; ‡, $p<0.05$ vs unloaded at day 7, two-way ANOVA with post hoc Holm test. (See Materials and Methods section for details).

Figure 3.
Effects of cyclic mechanical stretching of bovine bone marrow stromal cells (bMSC) on Runx2 (**A**) and PPARγ2 (**B**) protein levels at indicated days. Samples were either unstretched (open bars) or stretched (stripped bars) for 5 min. every day. Values are mean ± SEM of 6 wells per group expressed as a percentage of unloaded control (U). *: $p<0.05$ vs. unstretched, Mann-Whitney U test.

Figure 4.
Effects of cyclic mechanical stretching, Rosiglitazone or GW9662 treatment on the differentiation of C3H10T1/2 cells. (**A**) Representative photomicrographs (x 20) of C3H10T1/2 cells stained for alkaline phosphatase (elongated cells, empty arrows) and oil red O (round cells with dropplets, black arrows). Do note that in non treated conditions alkaline phosphatase-positive cells are abundant only in stretched cultures; in Rosiglitazone treated cells, lipid droplets are much more abundant, especially in unstretched cultures; under GW9662 treatment very few lipid droplets are seen. (**B**) Number of alkaline phosphatase positive cells and (**C**) number of oil red O positive cells at day 14 in unstretched (open bars) or stretched (stripped bars) cultures, treated or not with either Rosiglitazone or GW9662. Values are mean ± SEM of 6 wells per group. For clarity, only the most relevant significant differences (two-way ANOVA with post hoc Holm test) are labelled. *: $p<0.05$ vs matched unstretched cells; ‡: $p<0.05$ vs untreated and unstretched cells.

Figure 5.
Effects of cyclic mechanical stretching under Rosiglitazone or GW9662 treatment of C3H10T1/2 on *Runx2 and PPARγ2* mRNA levels. Cells were unstretched (open bars) or stretched (stripped bars)and treated or not with either Rosiglitazone or GW9662. Changes are expressed as percentage of unloaded control expression at day 3. (**A**) Expression of Runx2, (**B**) Expression of PPARγ2, at day 7 and day 14 of the culture. Values are mean ± SEM of 6 wells per group. For clarity, only the most relevant significant differences (two-way ANOVA with post hoc Holm test) are labelled. *: $p<0.05$ vs matched unstretched cells; ‡: $p<0.05$ vs untreated and unstretched cells.

Figure 6.
Effects of cyclic mechanical stretching under Rosiglitazone or GW9662 treatment of C3H10T1/2 cells on Runx2 and PPARγ2 activity at day 7. Cells were unstretched (open bars) or stretched (stripped bars) and treated or not with either Rosiglitazone or GW9662. Values are expressed as percentage of values for unstretched untreated cells (U). The graphs present the protein amounts of (**A**) Nuclear Runx2, (**B**) Osteocalcin, (**C**) Nuclear PPARγ2 and (**D**) PPARγ DNA binding activity. Values are mean ± SEM of 6 wells per group. For clarity, only the most relevant significant differences (two-way ANOVA with post hoc Holm test) are labelled. *: $p<0.05$ vs matched unstretched cells; ‡: $p<0.05$ vs untreated and unstretched cells.

Figure 7.
The effect of of mechanical stretching on PPARγ : proposed mechanism. Mechanical stretching promotes osteoblastogenesis by both upregulating Runx2 and downregulating PPARγ. Rosiglitazone-induced PPARγ activation promotes adipogenesis and decreases osteoblastogenesis whereas GW9662, a potent antagonist of PPARγ, induces the opposite. Mechanical stretching reduces the stimulation of adipogenesis and the inhibition of osteoblastogenesis induced by Rosiglitazone while increasing the osteoblastic stimulation induced by GW9662.

Tables

Table 1: Primers and conditions for real time PCR

Target gene	Species	θ m (°C)	A (s)	M (s)	Tm (°C)	Te (°C)	Forward	Reverse	Product size (pb)
RUNX2	bovine	58	7	14	70	68	accatggtggagatcatcg	tggggaggatttgtgaagac	325
OSX		58	7	14	70	68	cgggactcaacaactct	ccataggggtgtgtcat	308
OC		60	7	14	75	72	gcctttgtgtccaagc	ggaccccacatccatag	315
PPARγ2		52	5	10	72	65	aggatggggtcctcatatcc	gcgttgaacttcacagcaaa	132
aP2		58	5	10	72	62	agccactttcctggtagc	cttgtctccagtgaaaactt	111
L24		60	6	12	68	72	aggaaggctcaacgagaaca	caactcgaggagcagaaacc	231
RUNX2	mouse	55	5	10	65	60	tgtccttgtggattaaaaggacttg	tttagggcgcattcctcatc	102
OSX		55	5	10	72	63	cccttctcaagcaccaatgg	aagggtgggtagtcatttgcata	85
OC		60	5	10	72	65	acggtatcactatttaggacctgt	actttattttggagctgctgtgac	140
PPARγ2		58	5	10	65	65	cttcactgatacactgtctgc	gcattatgagacatccccac	112
aP2		58	8	16	65	65	cttgtctccagtgaaaactt	gtggaagtcacgcctttcat	347
ADD1		58	8	16	65	65	acggagccatggattgcaca	aagggtgcaggtgtcaccttt	422
Adipsin		55	5	10	64	60	tgcagtcgaaggtgtggttacg	gtgtctcttgtttccctgagc	170
L30		55	5	10	64	72	tttagaaaaaaggcctctac	caaacctgaatttccatgag	132

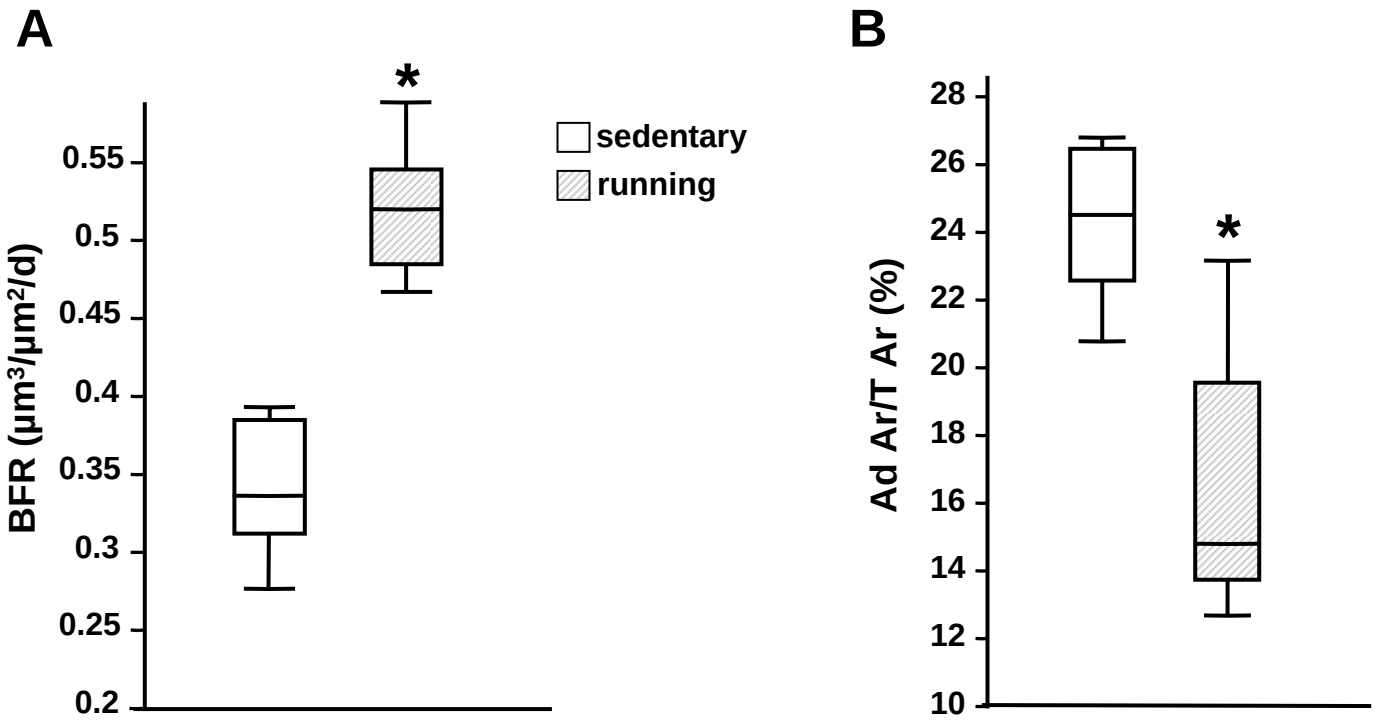

David et al, Fig. 1

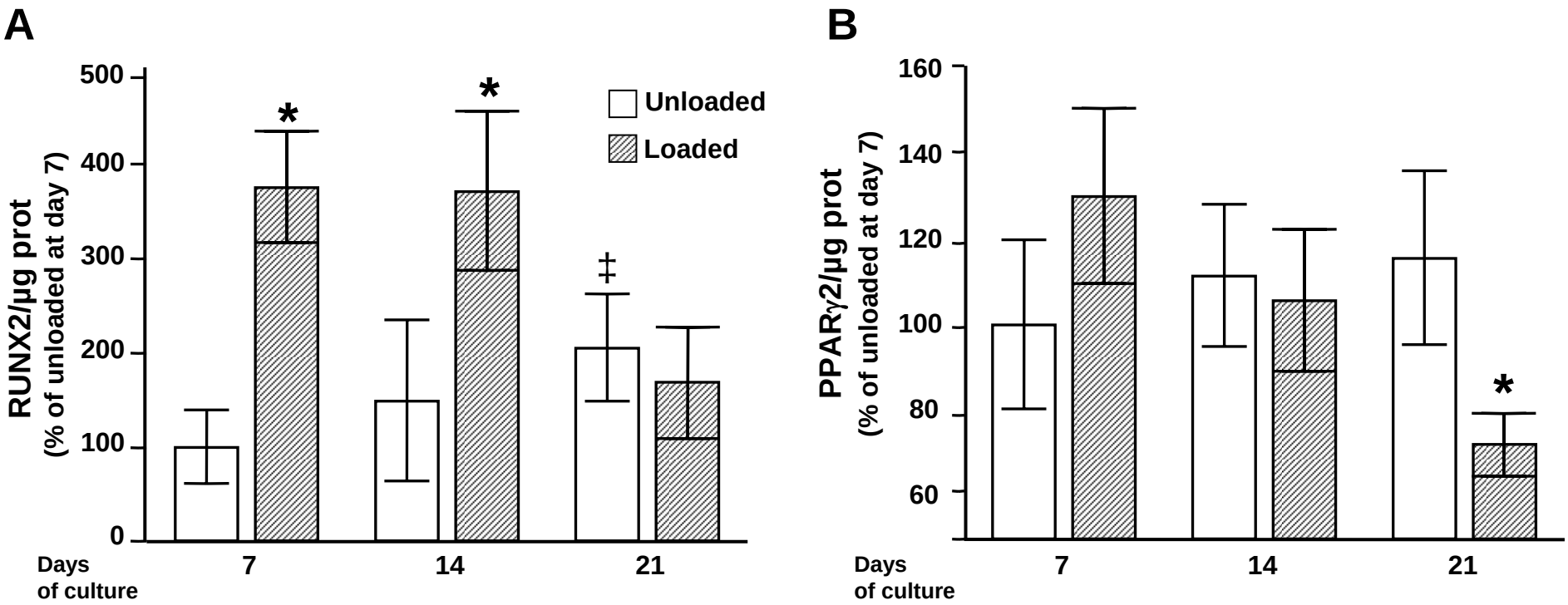

David et al., Fig. 2

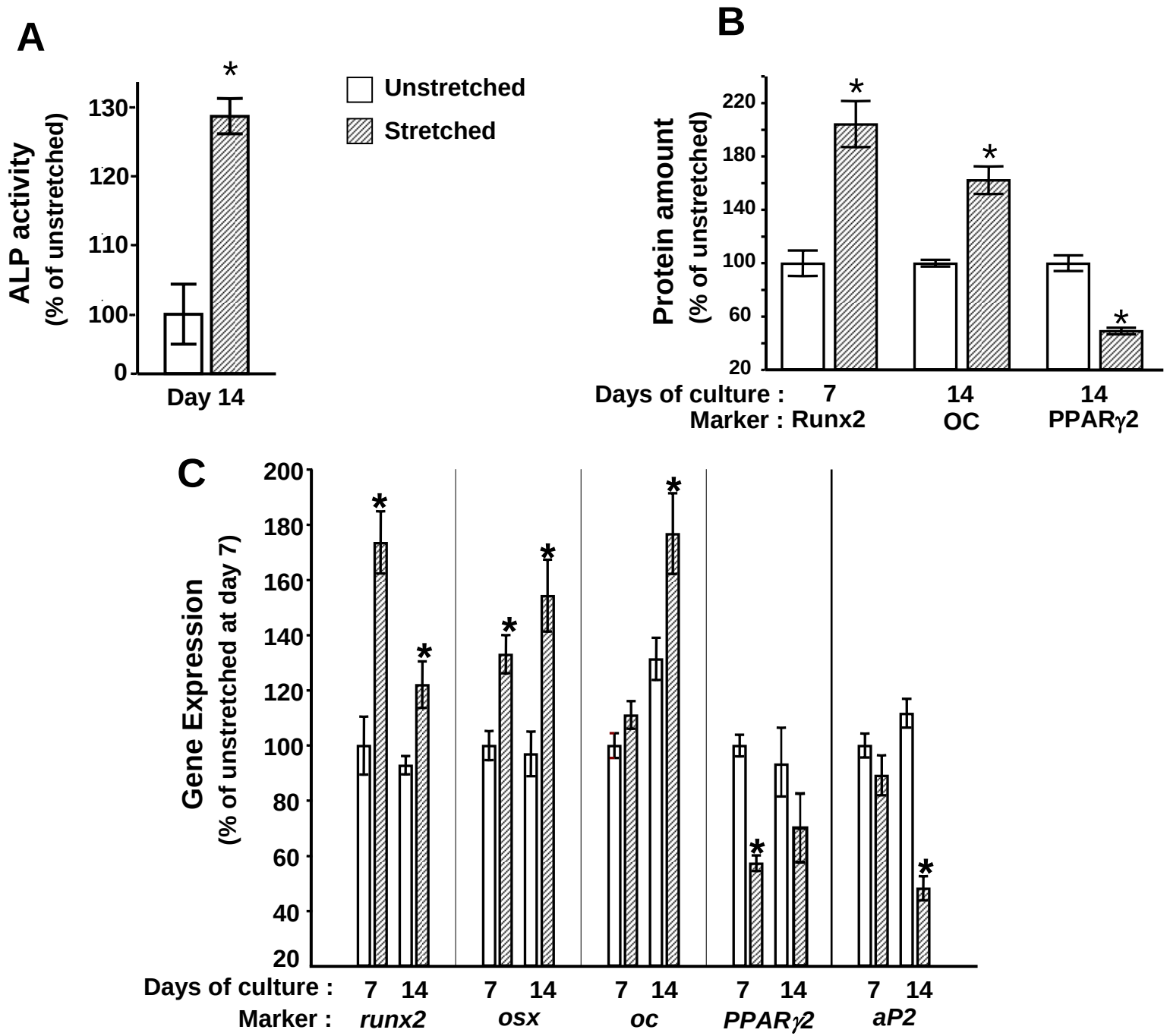

David et al., Fig. 3

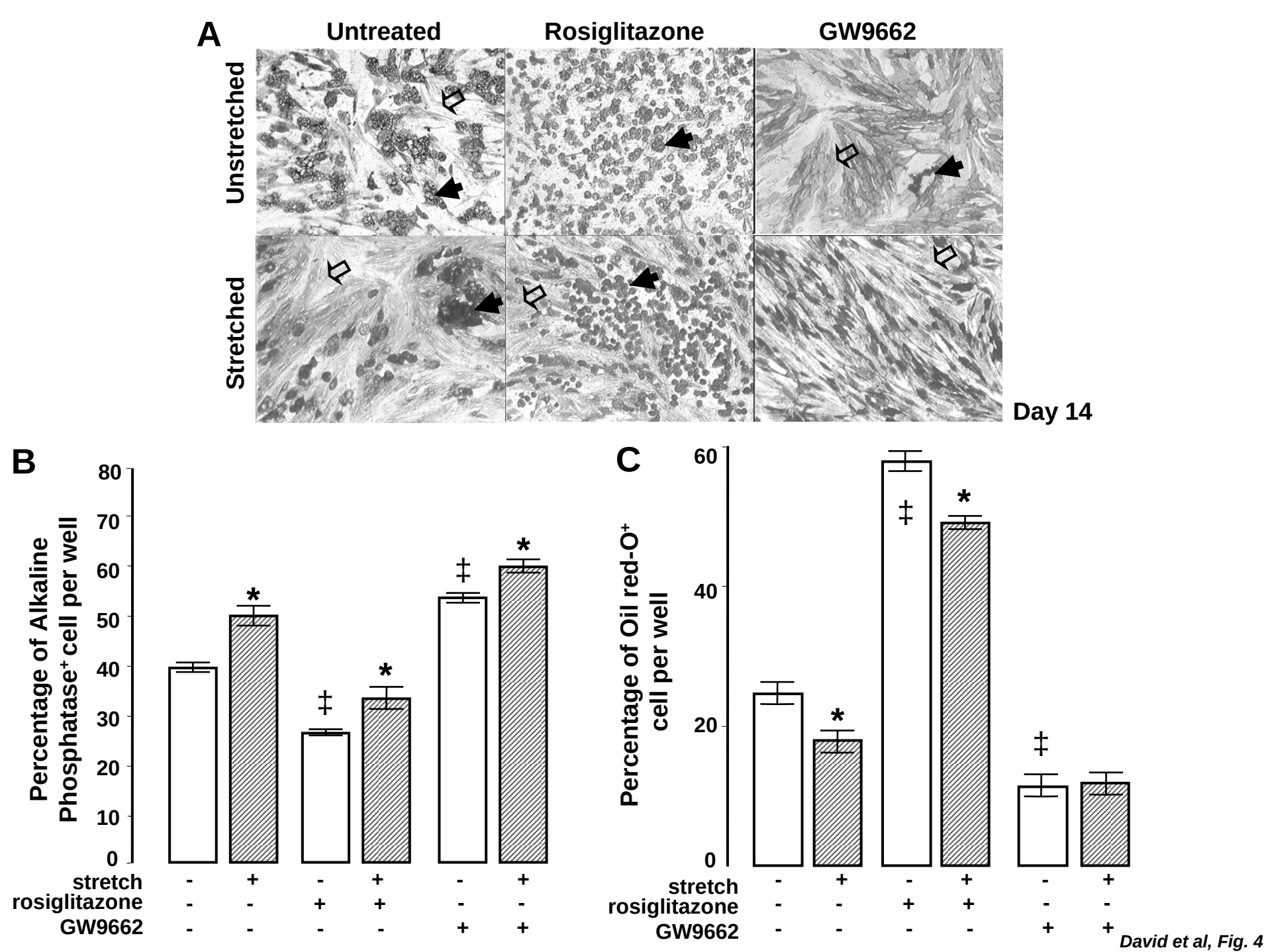
A
Untreated
Rosiglitazone
GW9662
Unstretched
Stretched
Day 14
B
Percentage of Alkaline Phosphatase+ cell per well
0
10
20
30
40
50
60
70
80
stretch - + - + - +
rosiglitazone - - + + - -
GW9662 - - - - + +
C
Percentage of Oil red-O+ cell per well
0
20
40
60
stretch - + - + - +
rosiglitazone - - + + - -
GW9662 - - - - + +
David et al, Fig. 4

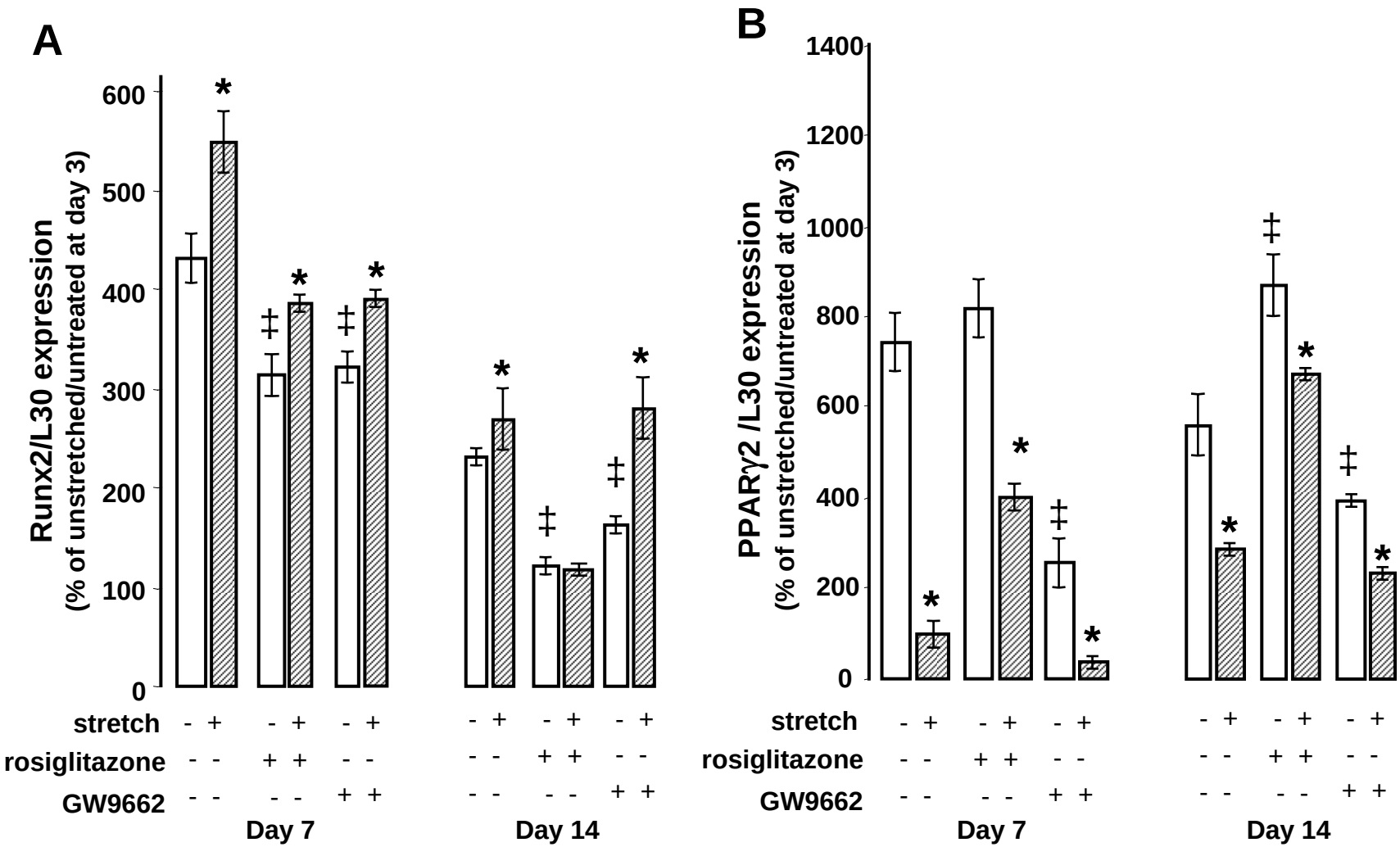

David et al., Fig. 5

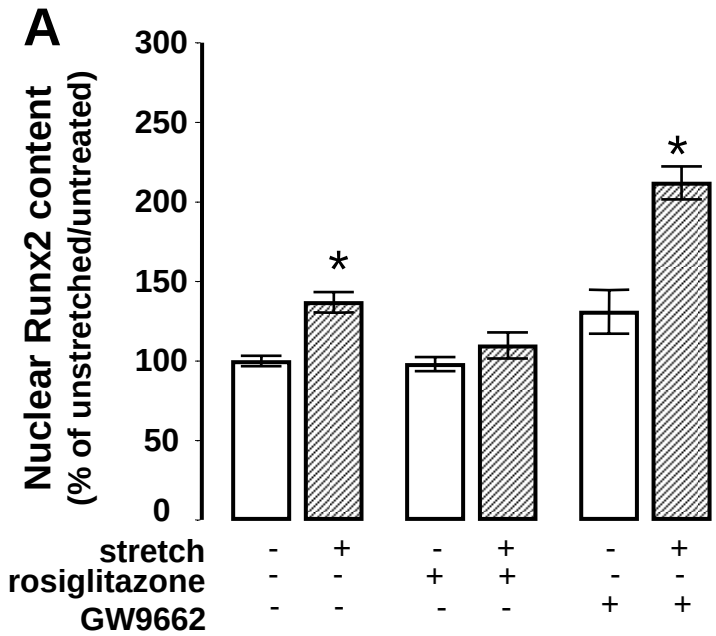

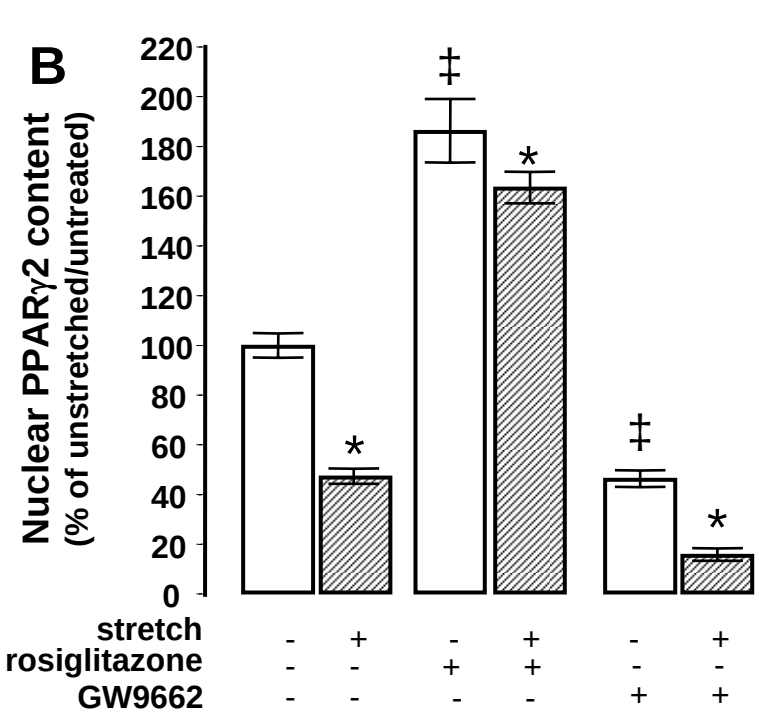

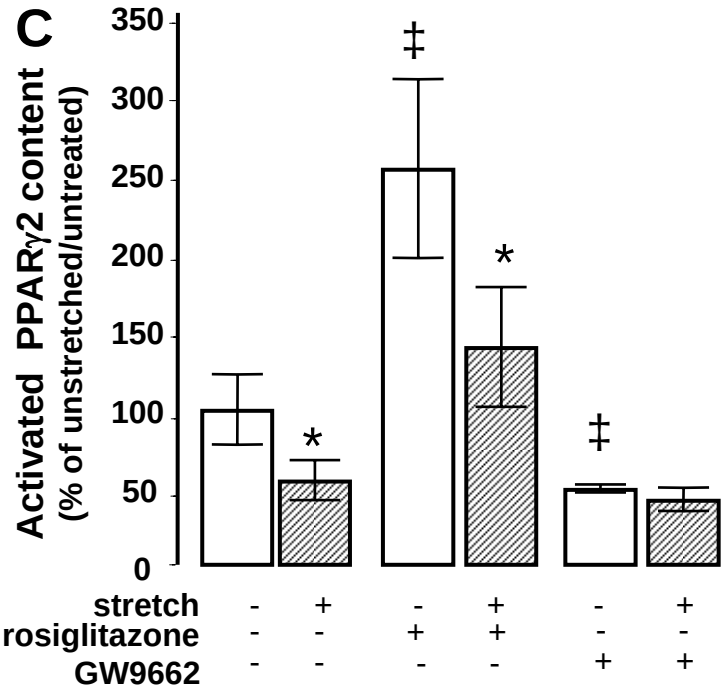

David et al., Fig. 6

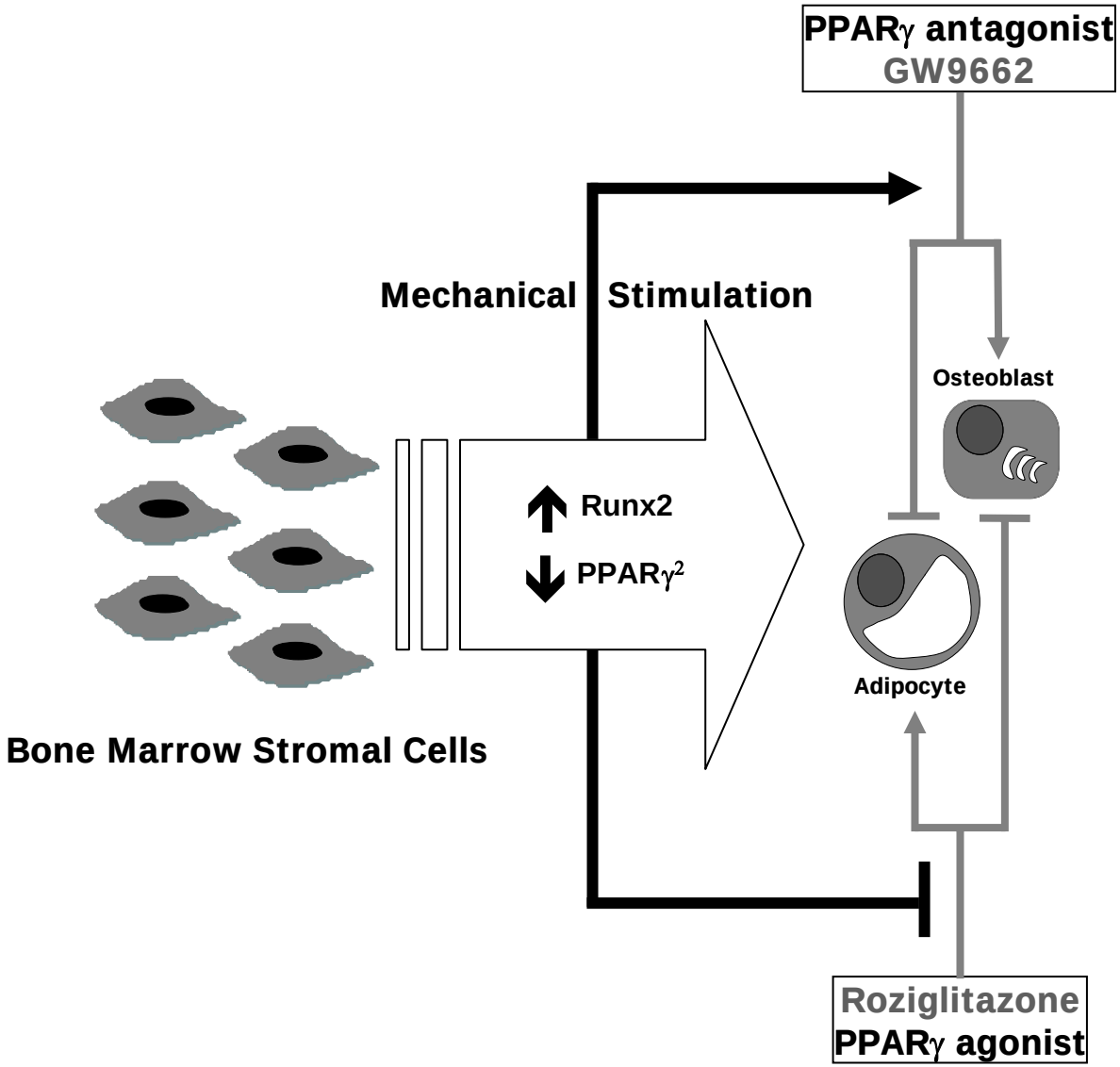

David et al, Fig. 7